# Fault Diagnosis of Analog Circuits Based on Machine Learning

Ke Huang, Haralampos-G. Stratigopoulos and Salvador Mir
TIMA Laboratory (CNRS-Grenoble INP-UJF), 46 Av. Félix Viallet, 38031 Grenoble, France

***Abstract*— We discuss a fault diagnosis scheme for analog integrated circuits. Our approach is based on an assemblage of learning machines that are trained beforehand to guide us through diagnosis decisions. The central learning machine is a defect filter that distinguishes failing devices due to gross defects (hard faults) from failing devices due to excessive parametric deviations (soft faults). Thus, the defect filter is key in developing a unified hard/soft fault diagnosis approach. Two types of diagnosis can be carried out according to the decision of the defect filter: hard faults are diagnosed using a multi-class classifier, whereas soft faults are diagnosed using inverse regression functions. We show how this approach can be used to single out diagnostic scenarios in an RF low noise amplifier (LNA).**

## I. Introduction

The design of integrated circuits (ICs) typically passes through many silicon iterations before it is finalized. Diagnosing the sources of failure in the first IC prototypes in a timely fashion is very critical to meet the time-to-market goal. Failure at this stage is related to the incomplete simulation models and the aggressive design techniques that are being adopted to exploit the maximum of performance out of the current technology.

A second application of fault diagnosis is in high-volume production where it can assist the designers in gathering information regarding the underlying failure mechanisms. This information constitutes valuable feedback to enhance yield in future product generations.

A comprehensive fault diagnosis method is also needed in cases where the IC is part of a larger system that is safety-critical (e.g. automotive, aerospace). During its lifetime, an IC might fail due to aging, wear-and-tear, harsh environments, overuse, or due to defects that are not detected by the production tests and manifest themselves later in the field of operation. Here, it is important to identify the root-cause of failure so as to repair the system if possible, gain insight about environmental conditions that can jeopardize the system's health, and apply corrective actions that will prevent failure reoccurrence and, thereby, expand the safety features.

Fault diagnosis is a severe challenge nowadays that calls for immediate solutions. Amongst the factors that inhibit diagnosis are the limited controllability and observability of internal blocks of ICs, the difficulty to de-embed internal components of blocks (i.e. reverse engineering), the difficulty to deal with unanticipated faults, the limited diagnostic information (only one/few IC samples showing the same erroneous behavior are available), and the fault ambiguity (i.e. different faults having the same influence on the IC behavior) which does not permit case-based reasoning.

In this paper, we propose a course of action for fault diagnosis in analog ICs. The key characteristic of our method is the use of a defect filter that offers a unified hard/soft fault diagnosis approach. Furthermore, soft fault diagnosis is achieved down to the transistor level, i.e. conclusions can be made as to which circuit branch, transistor or passive component is affected. The following section reviews previous work on analog circuit fault diagnosis. Section III describes our approach to answering the principal fault diagnosis questions. More specific diagnosis rules can be derived on a circuit by circuit case. This is illustrated with an example in section IV.

## II. Previous Work

Various types of fault diagnosis techniques have been proposed to date for analog circuits (a comprehensive review of techniques covering other circuits and systems can be found in [1]). They can be broadly categorized as rule-based, fault-model-based and behavioral-model-based.

### A. Rule-based diagnosis

Rule-based diagnostic systems represent the experience of skilled diagnosticians in the form of rules which generally take the form "IF symptom(s) THEN fault(s)" [2]. The main disadvantage of this approach is that it can only locate the faulty block in a larger system or an assembly fault (i.e. broken interconnect), but it cannot diagnose faulty components down to the transistor level.

### B. Fault-model-based diagnosis

Fault-model-based techniques require the *a priori* generation of fault hypotheses. In this step, an inductive fault analysis is combined with historical defect data to define a list of hard and soft fault hypotheses at the circuit netlist level.

Perhaps the most well-known fault-model-based technique is the fault dictionary [3], [4], [5]. A fault dictionary contains fault hypothesis/diagnostic measurement pattern pairs, which are generated by sequentially simulating the circuit, inserting each time a single fault in the netlist. The same diagnostic measurement pattern is obtained during diagnosis and is compared to those in the faulty dictionary using a similarity measure. The diagnosed fault is the one that pairs up with the most similar diagnostic measurement pattern. This is in essence a pattern recognition (e.g. classification) approach. As such, it is mostly suitable for catastrophic faults

978-3-9810801-6-2/DATE10 © 2010 EDAA

since parametric fault clusters tend to overlap when they are projected in a space of diagnostic measurements.

Soft faults can be diagnosed based on explicit nonlinear diagnosis equations of the form $F(p,m) = 0$, where $F$ is a matrix with elements that are nonlinear functions of the circuit parameters $p$ and diagnostic measurements $m$. Diagnosis equations can be derived analytically using a combination of component connection models, component transfer functions, and composite circuit transfer functions [6], [7]. Alternatively, they can be derived using statistical learning and regression [5], [8]. The solution $p^*$ to these equations can be reached using a Newton-Raphson iteration scheme, namely, $J_F\left(p^k\right)\left(p^{k+1}-p^k\right) = F\left(p^k,m\right)$, where $p^k$ is the $k$-th estimate of the solution and $J_F$ is the Jacobian of $F(p)$. This formulation goes along with diagnosability tests (i.e. ambiguity tests) to examine whether $p$ can be uniquely determined given $m$; however, no automated method exists to select diagnostic measurements that satisfy the diagnosability criterion. Moreover, it is not always guaranteed that the Newton-Raphson scheme will converge to a solution.

Soft faults can also be diagnosed based on linear error models [9], [10] of the form $\Delta m = S\left(\Delta p/p\right)$, where $\Delta p/p$ is the normalized vector of parameter deviations, $\Delta m$ is the vector of diagnostic measurement deviations, and $S$ is a sensitivity matrix evaluated at the nominal $p$. Thus, we can write $\Delta p/p = \left(S^TS\right)^{-1}S^T\Delta m$, provided that $\left(S^TS\right)^{-1}$ exists. However, in the presence of fault ambiguity, $S^TS$ is not full rank. Secondly, even with numerically full rank, $S^TS$ may still be nearly singular, in which case the solution will be unstable. Several algorithms have been proposed to determine fault ambiguity in this formulation resulting in a column-reduced sensitivity matrix with full rank [9], [11]. Clearly, linear error models are inadequate for substantial deviations of $p$. To address this issue, an iterative procedure is implemented that requires to update the sensitivity matrix at each step [9], [10]; however, there is no formal proof that guarantees convergence.

### C. Behavioral-model-based diagnosis

Behavioral-model-based techniques rely on generating an approximate behavioral model of the circuit [12], [13]. During fault diagnosis, this reference model is perturbed until its response matches the faulty response of the circuit. When a match is found, then a component which may have caused the failure is identified. The main difficulty with this approach is that the search towards a match can be computationally intensive.

### D. Test stimuli, diagnostic measurements extraction and selection

The generation of test stimuli and the extraction of diagnostic measurements are circuit-specific problems. Many proposals can be found in the literature for alternative test stimuli, including white noise [14] and power supply ramping [3]. Examples of alternative diagnostic measurements include identification curves [15] and wavelet decomposition [16]. In addition, several algorithms exist for selecting a minimal set of diagnostic measurements that covers all presumed faults [17], [18], [19].

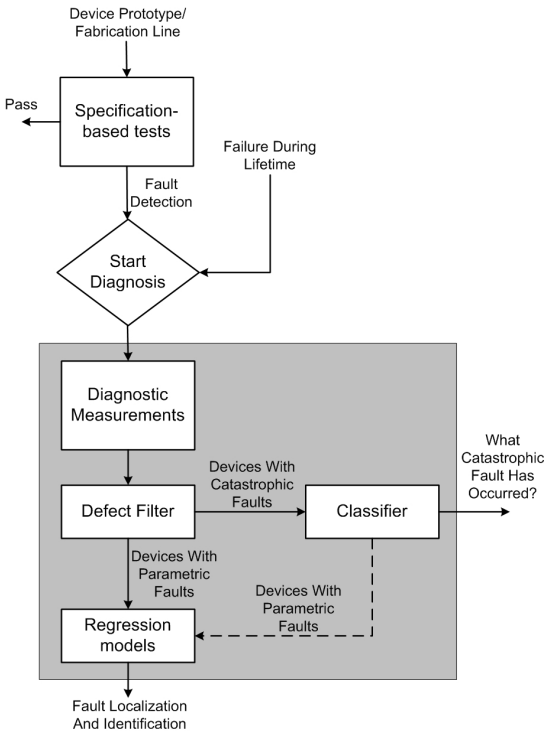


Fig. 1. Proposed fault diagnosis flow.

## III. Proposed Method

The proposed fault diagnosis method belongs to the fault-model-based category. It relies on an assemblage of learning machines that must be tuned in a pre-diagnosis learning phase. Learning machines have also been used in the past to implement an adaptive go/no go test [20]. A high-level description of the proposed method is illustrated in Fig. 1.

The diagnosis starts by obtaining the diagnostic measurements specified in the pre-diagnosis phase. At first, we can reside on a subset of the standard specification-based tests. If the diagnostic accuracy is not sufficient, the complete specification-based test suite can be used or additional special tests can be crafted to target undiagnosed parameters or to resolve ambiguity groups.

The central learning machine is a defect filter that is trained in the pre-diagnosis phase to distinguish devices with hard faults from devices with soft faults. Thus, the defect filter enables a unified hard/soft fault diagnosis approach without needing to specify in advance the fault type. We reuse here the defect filter proposed recently in the context of alternate test [21]. This filter relies on a non-parametric estimate $\tilde{f}\left(m\right)$ of the joint probability density function $f\left(m\right)$, where $m$ is the diagnostic measurements vector. By construction, it is parameterized with a single parameter $\alpha$, namely $\tilde{f}\left(m,\alpha\right)$, which can be tuned in the pre-diagnosis learning phase to control the extent of the filter, i.e. how much lenient or strict

it is in filtering out devices. The interested reader is referred to [21] for more details.

The defect filter forwards the device to the appropriate diagnosis tier according to the fault type that has been detected. If $\tilde{f}(m, \alpha) = 0$, then the device is inconsistent with the statistical nature of the bulk of the data that was used to estimate the density, thus it is considered to contain a hard fault. In this case, the device is forwarded to a classifier that is trained in the pre-diagnosis phase to map any diagnostic measurement pattern to the underlying hard fault. Thus, in this step we follow a fault dictionary approach that employs a multi-class classifier with $N$ outputs, where $N$ is the number of modeled catastrophic faults in the pre-diagnosis phase.

If $\tilde{f}(m, \alpha) > 0$, the device is considered to contain process variations, i.e. a soft fault has occurred. For soft fault diagnosis, we use nonlinear regression functions that are trained in the pre-diagnosis phase to map the diagnostic measurement pattern $m$ to the values of all internal circuit parameters of interest $p_j$, $j = 1, ..., n$ [22]. In particular, we train $n$ regression functions $f_j : m \mapsto p_j$. This approach allows to specify implicitly the unknown dependency between $m$ and all $p_j$ using statistical data and domain-specific knowledge. Thus, it avoids the complications related to an explicit formulation (i.e. diagnosability, convergence, problems with large deviations of $p$, etc.; see section II-B). The main goal is to construct regression models with generalization capabilities that can accurately diagnose future devices.

The defect filter is always tuned to filter out devices with catastrophic faults. However, this could inadvertently result in some devices with soft faults being also screened out and forwarded to the classifier. To correct this leakage, the classifier is trained during the pre-diagnosis phase to include detection of devices with process variations as well, i.e. an additional output is added, raising the number of outputs to $N + 1$. Thus, in the unlikely case where a device with a soft fault is presented to the classifier, the classifier kicks it back to the regression tier.

## IV. Case Study

### A. Low noise amplifier and its diagnostic measurements

Our case study is a 2.4 GHz LNA designed with the 0.25 $\mu$m BiCMOS7RF ST Microelectronics technology. The topology is shown in Fig. 2 and the specification requirements are listed in Table I. We have chosen the four scattering parameters as our initial diagnostic measurements (a DC diagnostic test will be added later to resolve one ambiguity that we found). Each scattering parameter is sampled at 41 frequency points between 1 GHz and 5 GHz with a step of 100 MHz. Thus, in total, we have $4 \times 41 = 164$ diagnostic measurements.

### B. Fault model

In a production environment (likewise in IC prototypes) global parametric deviations can be readily detected at wafer-level using process monitors in the scribe lines. Thus, for the purpose of diagnosis, our fault model includes (a) hard faults in the form of short and open circuits and (b) soft faults that

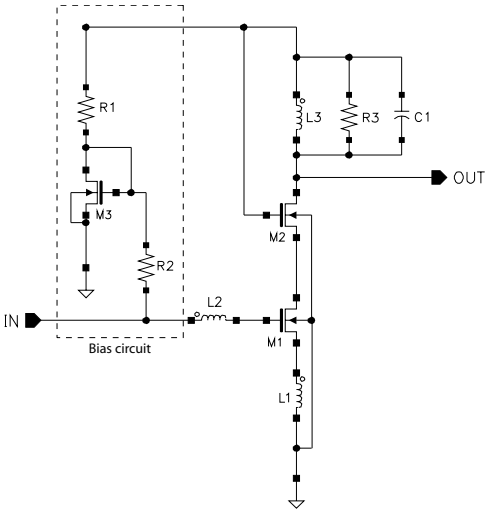


Fig. 2. Schematic of LNA under test.

TABLE I
PERFORMANCES AND SPECIFICATIONS FOR THE LNA UNDER TEST.

| NF (dB) | $S_{11}$ (dB) | $S_{12}$ (dB) | $S_{21}$ (dB) | $S_{22}$ (dB) | 1-dB CP (dBm) | $IIP_3$ (dBm) |
|---|---|---|---|---|---|---|
| $\leq 0.7$ | $\leq -8$ | $\leq -35$ | $\geq 11.5$ | $\leq -8.1$ | $\geq -3$ | $\geq 2.8$ |

account for location-dependent process deviations. Without doubt, the main disadvantage of fault-model-based diagnosis is that it cannot deal with unanticipated faults (see section II-B). Nevertheless, the set of simulated faults may be adequate for most diagnostic purposes. The definition of analog fault models is an on-going research topic and, certainly, success with this respect will also greatly benefit diagnosis tools.

We model short circuits in passive components and transistor terminals pairs with a 1 $\Omega$ resistor. Open circuits in the metal and polysilicon lines are modeled with a 10 M$\Omega$ resistor (an open at the gate of M3 is modeled by a broken trace since M3 operates in DC). In total, there are 23 hard faults, which are listed in Table II. In the abbreviation term $x\_XX\_yz$, $x$ denotes the hard fault type ($x$=$s$ for short circuit and $x$=$o$ for open circuit), $XX$ denotes the affected component, and $yz$ concerns only the transistors and denotes the terminals pair ($g$=gate, $d$=drain, and $s$=source).

We model soft faults as large deviations in the passive components and in the low-level transistor parameters (i.e. oxide thickness, substrate doping concentration, surface mobility, flatband voltage, etc.). Large parametric deviations in passive components are imposed by simply distorting their fault-free distribution to have a larger standard deviation. With respect to low-level transistor parameters, they are typically parameterized with a single variable $t$ with nominal value $t = 0$. Thus, denoting these parameters by $q_1, ..., q_k$, the transistor model consists of intricate functions of the form $q_i = f_i(t, q_1, ..., q_{i-1}, q_{i+1}, ..., q_k)$. A Monte Carlo simulation is then enabled by simply varying $t$ uniformly around $t = 0$ with standard deviation $\sigma_t$. This observation allowed us to generate realistic faulty transistor models by assigning a larger standard deviation $\beta_t \cdot \sigma_t$, $\beta_t > 1$. Intuitively, deviations in low-level transistor parameters will be reflected in the small-

TABLE II

LIST OF CATASTROPHIC FAULTS.

| *Fault* | *Faulty Component* |
|---|---|
| F1 | s_M3_gs, s_M3_ds |
| F2 | s_M1_ds |
| F3 | s_M1_gs |
| F4 | s_M1_gd |
| F5 | s_M2_ds |
| F6 | s_M2_gd, s_L3, s_R3, s_C1 |
| F7 | s_M2_gs |
| F8 | o_M3_d |
| F9 | o_M3_g |
| F10 | o_M3_s |
| F11 | o_M1_g, o_L2 |
| F12 | o_M1_s, o_L1 |
| F13 | o_M1_d, o_M2_s |
| F14 | o_M2_g |
| F15 | o_M2_d |
| F16 | s_R1 |
| F17 | s_R2 |
| F18 | s_L2 |
| F19 | s_L1 |
| F20 | o_R1, o_R2 |
| F21 | o_L3 |
| F22 | o_R3 |
| F23 | o_C1 |

TABLE III

LIST OF CIRCUIT PARAMETERS UNDER DIAGNOSIS.

| *Parameter* | *Nominal value* | *Fault-free distribution* | *Distorted distribution* | *RMS prediction error* |
|---|---|---|---|---|
| C1 | 500 fF | -5...5% | -40...40% | 3.6% |
| L1 | 700 pH | -5...5% | -40...40% | 3% |
| L2 | 8 nH | -5...5% | -40...40% | 2% |
| L3 | 6 nH | -5...5% | -40...40% | 2.7% |
| R1 | 2 KΩ | -5...5% | -40...40% | 22.5% |
| R2 | 3 KΩ | -5...5% | -40...40% | 19.7% |
| R3 | 100 Ω | -5...5% | -40...40% | 1% |
| $Cgs_1$ | 347 fF | -20.3...23% | -44.4...27.7% | 2.7% |
| $gm_1$ | 84 m | -20.3...42.6% | -94.1...79.7% | 2% |
| $Cgs_2$ | 358 fF | -13.8...17.7% | -34.5...20.8% | 2.7% |
| $gm_2$ | 87 m | -18.8...34.5% | -94...70.6% | 2% |
| $Cgs_3$ | 52 fF | -19.2...22.4% | -22.1...24.4% | 3% |
| $gm_3$ | 10 m | -13.1...16.3% | -26.1...42.3% | 11.5% |

signal parameters. To this end, we deemed efficient to monitor deviations in $g_m$ and $C_{gs}$.

The first column of Table III summarizes the circuit parameters that we diagnose in our experiment (13 in total). The second column lists their nominal values. The third column shows minimum and maximum parameter variations observed over 5000 Monte Carlo simulations using nominal standard deviations. The forth column shows the corresponding parameter variations after having increased the standard deviations. It should be noted that the distortions that we have imposed in the parameters distributions are illustrative and can be changed to accommodate any fault model of this type.

### C. Classifier and regression functions

We use a support vector machine (SVM) classifier [23]. In contrast to other type of classifiers (i.e. neural networks, nearest neighbors, etc.), SVMs allocate the separation boundaries such that they traverse the middle of the distance between the fault clusters. Now, as will be shown later, our fault clusters are cleanly separated when they are projected in the diagnostic measurement space, i.e. there are large empty subspaces amidst the fault clusters. This means that SVMs will be insensitive to measurement noise or even equipment drifts. In addition, SVMs ensure that complexity is controlled independently of the number of diagnostic measurements. SVMs can be adapted for regression as well [23]. In this experiment, we used the *Kernel-based Machine Learning Lab* package [24] in the *R Project* (www.r-project.org) to implement both the classifier and the regression functions based on SVMs.

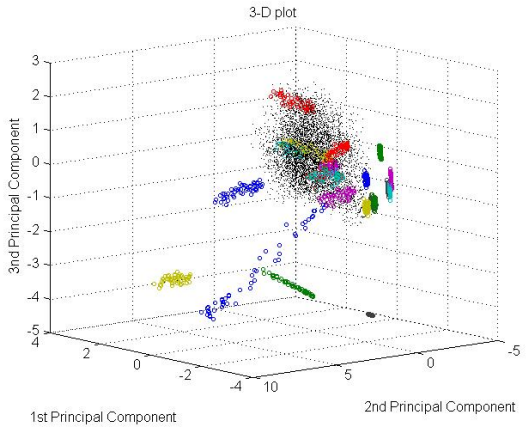


Fig. 3. Projection of training devices in the top three principal components.

### D. Pre-diagnosis learning phase

We generate the following data sets to train and validate the learning machines (e.g. defect filter, classifier, regression functions) of the diagnosis flow:

- The set $S_1$ contains 10000 LNA instances generated by Monte Carlo simulation where all circuit parameters are sampled from their distorted distributions in Table III. The hint here is to model larger component variations in the pre-diagnosis phase than those expected in reality. This way, we minimize the probability that the defect filter will screen out devices with excessive parametric deviations and we ensure that future devices will fall in regions where the regression functions are valid, i.e. in regions where there were enough samples during the pre-diagnosis phase to carry out the regression. In other words, $S_1$ must be information-rich such that the learning machines can generalize for every possible fault scenario.
- The set $S_2$ contains 23 subsets $S_{2j}$, $j = 1, ..., 23$, corresponding to the 23 fault classes in Table II. Each subset $S_{2j}$ contains 100 LNA instances generated by inserting the hard fault $j$ in the netlist and subsequently running 100 Monte Carlo simulations where the rest of the circuit parameters are sampled from their fault-free distributions. Thus, the size of $S_2$ is $23 \times 100 = 2300$.

To gain some insight about the structure of the data, we perform a Principal Component Analysis (PCA) on the (10000+2300)×164 matrix whose rows correspond to the

diagnostic measurement patterns of the devices in $S_1$ and $S_2$. Fig. 3 shows the projection of these devices in the top three principal components. Fault clusters are represented with different colors, whereas the largely populated "process variation" class is represented with black dots. As can be observed, even in this primitive visualization, fault clusters are cleanly separated.

The set $S_1$ is split in two equal sets $S_1^t$ and $S_1^v$ uniformly at random. Similarly, $S_2$ is split in $S_2^t$ and $S_2^v$.

$S_1^t$ is used to built the defect filter, i.e. to generate the density estimate $\tilde{f}(m, \alpha)$. $S_1^v$ and $S_2$ are used to validate the defect filter. We tested a defect filter with $\alpha = 0$ (this value of $\alpha$ implements a rather strict defect filter, see [21]) which gave optimal filtering: devices in $S_2$ have a zero density while devices in $S_1^v$ have a nonzero density.

The regression models are trained using $S_1^t$ and are validated using $S_1^v$. The result is shown in the fifth column of Table III in terms of the RMS prediction error. As can be observed, the regression models can predict accurately multiple parameter variations with the exception of the resistors $R_1$, $R_2$ and the transistor M3 in the bias circuit. In retrospect, this could have been anticipated because the bias circuit operates in DC, thus it is not excited by the high-frequency diagnostic measurements. As we will see later, this results in an ambiguity, which calls for additional diagnostic measurements.

The classifier is trained using $S_1^t$ and $S_2^t$ and is validated using $S_1^v$ and $S_2^v$ ($S_1$ constitutes the "process variations" class). The only misclassification occurred between fault classes F8 and F9. Looking at the LNA schematic, it can be observed that faults F8 and F9 have the same effect: the transistor M3 is off. Thus, these two fault classes can be collapsed in one, resulting in an overall 100% classification rate. This example illustrates that the classifier can help us to identify ambiguous hard faults in the pre-diagnosis phase that we missed out by just looking at the schematic with the naked eye.

### *E. Diagnosis phase*

The efficiency of the proposed diagnosis flow to predict multiple parameter variations is verified by the fifth column of Table III. Next, we evaluate the generalization of the diagnosis flow for the case of single faults. We use the following data sets:

- The set $S_3$ is generated independently in the same way as $S_2$. This set corresponds to 23 single hard fault scenarios.
- The set $S_4$ contains 20 subsets $S_{4j}$, $j = 1, ..., 20$, corresponding to the 20 single soft fault scenarios shown in the first column of Table IV. For the passive components, we consider $\pm 30\%$ deviations. For the transistors, we distort the mean value of $t$ in two directions (for transistor MX, MX+ means positive direction and MX- means negative direction) such that the inflicted (excessive) variations on $g_m$ and $C_{gs}$ are still within the ranges of the fourth column of Table III. Each subset $S_{4j}$ contains 100 LNA instances generated by inserting the $j$-th single soft fault and running 100 Monte Carlo simulations where the rest of (unaffected) parameters are sampled from their fault-free distribution. Thus, the size of $S_4$ is $20 \times 100 = 2000$.

TABLE IV
SINGLE SOFT FAULT SCENARIOS.

| *Single fault scenarios* | *Number of faulty circuits /100* | *RMS error of estimated values* |
|---|---|---|
| C1+30% | 69 | 1.9% |
| C1-30% | 0 | - |
| L1+30% | 74 | 1.5% |
| L1-30% | 0 | - |
| L2+30% | 17 | 1.9% |
| L2-30% | 81 | 1.9% |
| L3+30% | 88 | 1.5% |
| L3-30% | 0 | - |
| R1+30% | 0 | - |
| R1-30% | 0 | - |
| R2+30% | 0 | - |
| R2-30% | 0 | - |
| R3+30% | 100 | 0.6% |
| R3-30% | 42 | 1.3% |
| M1+ | 19 | $cgs_1$ : 2.4%<br>$gm_1$ : 1.2% |
| M1- | 4 | $cgs_1$ : 1%<br>$gm_1$ : 1% |
| M2+ | 0 | - |
| M2- | 0 | - |
| M3+ | 16 | $cgs_3$ : 1.9%<br>$gm_3$ : 5% |
| M3- | 94 | $cgs_3$ : 3.2%<br>$gm_3$ : 3% |
| **Total** | 604/2000 | - |

The devices in $S_3$ and $S_4$ undergo specification-based testing, according to Fig. 1. All devices in $S_3$ violate at least one specification and as such are labeled as faulty. However, this is not the case for devices in $S_4$, as shown in the second column of Table IV. Faulty devices are next forwarded to the diagnosis phase where they are first subjected to the defect filter. The defect filter fails to characterize correctly a single device with parametric fault L2+30%, which is erroneously screened out and forwarded to the classifier. However, the classifier maps it to the "process variation" class and kicks it back to the regression tier as indicated by the dashed arrow in Fig. 1. The rest of devices with catastrophic faults are all correctly classified, thus we conclude that catastrophic fault diagnosis succeeds 100%.

All faulty devices in $S_4$ are forwarded to the regression tier. The third column of Table IV shows the RMS prediction error of the parameters that deviate in each fault scenario and Fig. 4 plots the situation for L2 and R3. Notice that the RMS prediction error of the "fault-free" parameters (not shown here due to lack of space) is similar to this of Table III (in general it is even smaller since large errors typically correspond to excessive deviations).

The following observations are useful in building soft fault diagnosis rules: (a) the deviations of $g_{m1}$ and $g_{m2}$ are not necessarily due to a fault in M1 or M2. Indeed, $g_{m1}$ and $g_{m2}$ depend on the current flowing through M1 and M2, which, in turn, depends on all passive components in the same branch, as well as on the bias circuit. Thus, a fault in any passive component or in the bias circuit will also impact $g_{m1}$ and

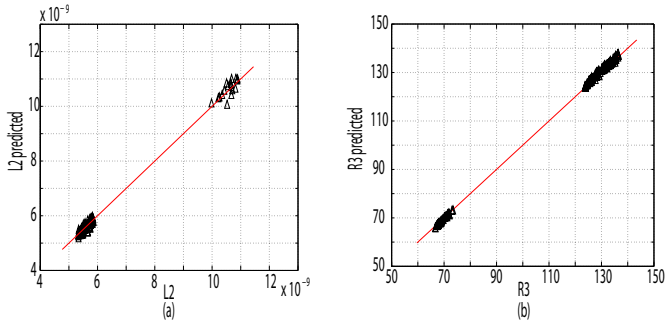


Fig. 4. Comparison between target and predicted values. Each scatter point corresponds to a faulty instance. Ideally these points should fall on the 45° line.

$g_{m2}$. (b) A soft fault in M2 does not render the circuit faulty (see zero M2 entries in Table IV). (c) Recall from section IV-D that the components of the bias circuit cannot be diagnosed by high-frequency measurements; hence, the predicted deviations of R1, R2, or M3 are not genuine and, thereby, are disregarded. (d) The probability of two soft faults occurring at the same time is negligible.

Based on the above observations, we define the following diagnosis rules: (a) if both $g_{m1}$ and $g_{m2}$ deviate and at the same time a passive component deviates, then the passive component is faulty. (b) If only $g_{m1}$ and $g_{m2}$ deviate, then the faulty component is M1 or is located in the bias circuit. The latter rule leads to the only ambiguity so far. Now, notice that the LNA fails if a fault within the bias circuit results in a dramatic decrease of the DC bias point of M1 and/or the input impedance of the bias circuit. Thus, this ambiguity can be resolved in part by measuring the gate-source voltage $V_{gs3}$ of M3 (the gate of M3 is not an RF sensitive node). Two follow-up rules to rule (b) above are: (c) if $g_{m1}$ deviates and $V_{gs3}$ is outside its tolerance, then M3 is faulty, (d) if $g_{m1}$ deviates and $V_{gs3}$ is within its tolerance, then the faulty component is M1 or is located in the bias circuit. Using rule (c), we were able to diagnose correctly 49 out of the 16+94=110 circuits with faulty M3.

## V. Conclusions

We presented a fault diagnosis method that relies on learning machines to answer the principal questions posed in a branching diagnosis flow. A defect filter detects the type of fault (hard or soft) and forwards the faulty device to the appropriate tier. Devices with hard faults are diagnosed using a multi-class classifier. If the fault that occurred is soft, then inverse regression functions are used to predict simultaneously a set of predefined design and transistor-level parameters, in order to locate the faulty parameter and identify its value. In general, some auxiliary circuit-specific fault diagnosis rules are required to resolve ambiguities. This was demonstrated with an LNA example with high overall diagnosis success.

## Acknowledgments

This research has been carried out with the support of a Marie Curie International Reintegration Grant (CT-2007-209653) and the European CATRENE project CT302-TOETS.

## References

[1] W. Fenton, T. M. McGinnity, and L. P. Maguire, "Fault diagnosis of electronic systems using intelligent techniques: A review," *IEEE Trans. Syst., Man, Cybern. C, Appl. Rev.*, vol. 31, no. 3, pp. 269–281, 2001.

[2] E. S. Erdogan, S. Ozev, and P. Cauvet, "Diagnosis of assemply failures for system-in-package RF tuners," in *Proc. IEEE Int. Symp. Circuits Syst.*, 2008, pp. 2286–2289.

[3] S. S. Somayajula, E. Sanchez-Sinencio, and J. Pineda de Gyvez, "Analog fault diagnosis based on ramping power supply current signature clusters," *IEEE Trans. Circuits Syst. II, Analog Digit. Signal Process.*, vol. 43, no. 10, pp. 703–712, 1996.

[4] Y. Maidon, B. W. Jervis, N. Dutton, and S. Lesage, "Diagnosis of multifaults in analogue circuits using multilayer perceptrons," *Proc. Inst. Electr. Eng. - Circuits Devices Syst.*, vol. 144, no. 3, pp. 149–154, 1997.

[5] S. Chakrabarti, S. Cherubal, and A. Chatterjee, "Fault diagnosis for mixed-signal electronic systems," in *Proc. IEEE Aerosp. Conf.*, 1999, pp. 169–179.

[6] N. Sen and R. Saeks, "Fault diagnosis for linear systems via multifrequency measurements," *IEEE Trans. Circuits Syst.*, vol. 26, no. 7, pp. 457–465, 1979.

[7] L. Rapisarda and R. A. Decarlo, "Analog multifrequency fault diagnosis," *IEEE Trans. Circuits Syst.*, vol. CAS-30, no. 4, pp. 223–234, 1983.

[8] S. Cherubal and A. Chatterjee, "Test generation based diagnosis of device parameters for analog circuits," in *Proc. Des. Autom. Test Eur.*, 2001, pp. 596–602.

[9] H. Dai and M. Souders, "Time-domain testing strategies and fault diagnosis for analog systems," *IEEE Trans. Instrum. Meas.*, vol. 39, no. 1, pp. 157–162, 1990.

[10] M. Slamani and B. Kaminska, "Analog circuit fault diagnosis based on sensitivity computation and functional testing," *IEEE Des. Test Comput.*, vol. 9, no. 1, pp. 30–39, 1992.

[11] G. J. Hemink, B. W. Meijer, and H. G. Kerkhoff, "Testability analysis of analog systems," *IEEE Trans. Comput.-Aided Des.*, vol. 9, no. 6, pp. 573–583, 1990.

[12] E. F. Cota, M. Negreiros, L. Carro, and M. Lubaszewski, "A new adaptive analog test and diagnosis system," *IEEE Trans. Instrum. Meas.*, vol. 49, no. 2, pp. 223–227, 2000.

[13] E. Simeu and S. Mir, "Parameter identification based diagnosis in linear and nonlinear mixed-signal systems," in *Proc. Int. Mixed-Signals Test. Workshop*, 2005, pp. 140–147.

[14] R. Spina and S. Upadhyaya, "Linear circuit fault diagnosis using neuromorphic analyzers," *IEEE Transactions on Circuits and Systems-II: Analog and Digital Signal Processing*, vol. 44, no. 3, pp. 188–196, 1997.

[15] Z. Czaja, "Using a square-wave signal for fault diagnosis of analog parts of mixed-signal electronic embedded systems," *IEEE Trans. Instrum. Meas.*, vol. 57, no. 8, pp. 1589–1595, 2008.

[16] M. Aminian and F. Aminian, "A modular fault-diagnosis system for analog electronic circuits using neural networks with wavelet transform as a preprocessor," *IEEE Trans. Instrum. Meas.*, vol. 56, no. 5, pp. 1546–1554, 2007.

[17] S. Mir, M. Lubaszewski, and B. Courtois, "Fault-based ATPG for linear analog circuits with minimal size multifrequency test sets," *J. Electron. Test.: Theory Appl.*, vol. 9, no. 1-2, pp. 43–57, 1996.

[18] J. A. Starzyk, D. Liu, Z. H. Liu, D. E. Nelson, and J. O. Rutkowski, "Entropy-based optimum test points selection for analog fault dictionary techniques," *IEEE Trans. Instrum. Meas.*, vol. 53, no. 3, pp. 754–761, 2004.

[19] H.-G. Stratigopoulos, P. Drineas, M. Slamani, and Y. Makris, "Non-RF to RF test correlation using learning machines: A case study," in *IEEE VLSI Test Symp.*, 2007, pp. 9–14.

[20] H.-G. Stratigopoulos and Y. Makris, "Error moderation in low-cost machine-learning-based Analog/RF testing," *IEEE Trans. Comput.-Aided Des. Integr. Circuits Syst.*, vol. 27, no. 2, pp. 339–351, 2008.

[21] H.-G. Stratigopoulos, S. Mir, E. Acar, and S. Ozev, "Defect filter for alternate RF test," in *Proc. IEEE Eur. Test Symp.*, 2009, pp. 101–106.

[22] S. Bhattacharya and A. Chatterjee, "A fast process diagnosis method using diagnosis core," in *Proc. Int. Mixed-Signals Test. Workshop*, 2003, pp. 19–24.

[23] N. Cristianini and J. Shawe-Taylor, *Support Vector Machines and Other Kernel-Based Learning Methods*, Cambridge, 2000.

[24] A. Karatzoglou, A. Smola, K. Hornik, and A. Zeileis, "An S4 package for kernel methods in R," *J. Stat. Softw.*, vol. 11, no. 9, pp. 1–20, 2004.